

# Multi-harmonic approach to determine load dependent local flux variations in power transformer cores\*

BJÖRN RIEMER, KAY HAMEYER

*RWTH Aachen University  
 Institute of Electrical Machines  
 Schinkelstraße 4, 52056 Aachen, Germany  
 e-mail: bjoern.riemer@iem.rwth-aachen.de*

(Received: 30.09.2014, revised: 15.10.2014)

**Abstract:** This paper presents a methodology for the calculation of the flux distribution in power transformer cores considering nonlinear material, with reduced computational effort. The calculation is based on a weak coupled multi-harmonic approach. The methodology can be applied to 2D and 3D Finite Element models. The decrease of the computational effort for the proposed approach is >90% compared to a time-stepping method at comparable accuracy. Furthermore, the approach offers a possibility for parallelisation to reduce the overall simulation time. The speed up of the parallelised simulations is nearly linear. The methodology is applied to a single-phase and a three-phase power transformer. Exemplary, the flux distribution for a capacitive load case is determined and the differences in the flux distribution obtained by a 2D and 3D FE model are pointed out. Deviations are significant, due to the fact, that the 2D FE model underestimates the stray fluxes. It is shown, that a 3D FE model of the transformer is required, if the non-linearity of the core material has to be taken into account.

**Key words:** flux distribution, local flux variations, multi-harmonic FEM, nonlinear FEM, power transformer

## 1. Introduction

Power transformers are counted among the most important components in the energy transmission grid. Due to its continuous operation, a high efficiency is indispensable. Amongst others, the losses of transformers depend on stray fluxes and its local distribution. According to the load, the superposition of exciting and stray flux can lead to significant local flux variations in the core, especially for transformers with large short circuit impedances, e.g. phase-shifting transformers.

---

\* This is extended version of paper which was presented at the 23th Symposium on Electromagnetic Phenomena in Nonlinear Circuits, Pilsen, Czech Republic 02-04.07.2014. Professor Ivo Doležel was chairman of organizing committee

Since saturation of the core definitely has to be avoided, possible load dependent local flux variations have to be considered already in the design stage. Several approaches to model the magnetic load of transformer cores are given in the literature. Magnetic equivalent circuits offer a computationally efficient way to calculate the main behaviour of a transformer. However, the local resolution of stray flux paths is rather low. The finite element method (FEM) increases the accuracy of the calculated flux distribution. In general, power transformers have distinctive three-dimensional structure and stray flux paths. 3D FEM represents the transformer geometry and the flux paths accurately. However, a 3D nonlinear FEM requires a high computational effort.

In general, the voltage defines the transformers working point. Thus, a voltage driven simulation is necessary. Considering a time-stepping simulation the transient phenomenon has to decay, before the steady state can be analysed. This can be a challenge, due to quite large time constants of power transformers.

A well-known alternative approach for steady state analysis is a nonlinear time-harmonic simulation. This approach considers only the fundamental component of the electrical and magnetic quantities. An effective B-H characteristic, which can be adapted based on the magnetic energy, represents the core material [1]. The harmonic balance finite element method accounts for a defined set of higher harmonics in a single computational step [2]. [3] presents a strong-coupled multi-harmonic approach. The finite element formulation is transferred into the frequency domain and a technical relevant set of harmonics is incorporated into the system matrix. The method has a lower computational effort when compared to a time stepping approach. Nevertheless, there are some disadvantages of this method. A drawback of this method is the complexity of the strong-coupled spatial discretisation and the considered frequency domains. The system matrix increases with the number of selected harmonics. This can be a limitation especially for 3D models of large power transformers.

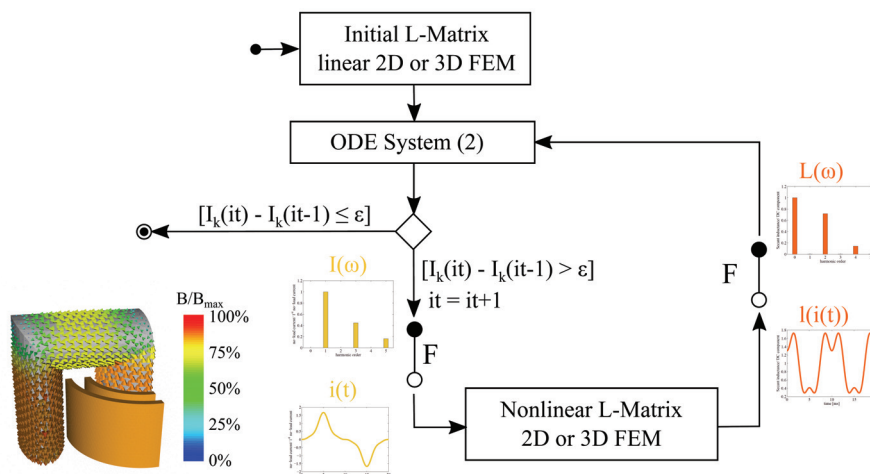


Fig. 1. Flow chart of the multi-harmonic determination of the working point

This paper presents a weak coupled multi-harmonic approach. A set of differential equations represent the transformers behaviour in the frequency domain, whereas the transformers lumped parameters are determined by means of static nonlinear Finite Element computations in the time-domain.

First, this paper figures out the theoretical framework of the proposed approach. The approach is applied to determine the no load operation of a single-phase and a three-phase transformer. Both, 2D and 3D models of the transformer are used. For validation purposes, the results and the computational effort of the multi-harmonic approach are compared to a time-stepping method. Finally, the proposed method is applied to analyse the magnetic flux distribution inside the core of a three-phase five-limb transformer for a capacitive load case by means of 2D and 3D FE model of the transformer.

## 2. Theoretical framework

Lumped parameters, and therefore, the differential Equations (1) represent the transformer:

$$\mathbf{u}(t) = \mathbf{r} \cdot \mathbf{i}(t) + \frac{d}{dt} \psi(\mathbf{i}, t), \quad (1)$$

with phase voltages  $\mathbf{u}(t)$ , winding resistance matrix  $\mathbf{r}$ , phase currents  $\mathbf{i}(t)$ , flux linkage matrix  $\psi(\mathbf{i}, t) = \mathbf{I}(\mathbf{i}(t)) \cdot \mathbf{i}(t)$  and secant inductance matrix  $\mathbf{I}(\mathbf{i}(t))$ . Transformation of differential Equation (1) into the frequency domain and redirection with respect to the currents yields:

$$\tilde{\mathbf{I}} = [\tilde{\mathbf{R}} + j\omega \tilde{\mathbf{L}}]^{-1} \cdot \tilde{\mathbf{U}}, \quad (2)$$

with the resistance matrix:

$$\tilde{\mathbf{R}} = \begin{pmatrix} \mathbf{R}(0) & \cdots & \mathbf{R}(M-1) \\ \vdots & \ddots & \vdots \\ \mathbf{R}(M-1) & \cdots & \mathbf{R}(0) \end{pmatrix}, \quad (3)$$

the inductance matrix:

$$\tilde{\mathbf{L}} = \begin{pmatrix} 0 \cdot \mathbf{L}(0) & \cdots & 0 \cdot \mathbf{L}(M-1) \\ \vdots & & \vdots \\ \frac{M}{2} \cdot \mathbf{L}\left(\frac{M}{2}\right) & \ddots & \vdots \\ \left(1 - \frac{M}{2}\right) \cdot \mathbf{L}\left(\frac{M}{2} + 1\right) & \ddots & \vdots \\ \vdots & & \vdots \\ -1 \cdot \mathbf{L}(M-1) & \cdots & -1 \cdot \mathbf{L}(0) \end{pmatrix}, \quad (4)$$

the voltages and currents:

$$\tilde{\mathbf{U}} = \begin{pmatrix} \mathbf{U}(0) \\ \vdots \\ \mathbf{U}(M-1) \end{pmatrix} \text{ and } \tilde{\mathbf{I}} = \begin{pmatrix} \mathbf{I}(0) \\ \vdots \\ \mathbf{I}(M-1) \end{pmatrix}, \quad (5)$$

and the considering discrete Fourier coefficients of the voltages, currents, resistances and inductances:

$$\mathbf{X}(k) = \sum_{n=1}^{M-1} \mathbf{x}(n) \cdot e^{-j \cdot 2\pi k F_n}, \quad k = 0 \dots M-1, \quad \mathbf{x} \in (\mathbf{u}, \mathbf{i}, \mathbf{r}, \mathbf{l}). \quad (6)$$



Fig. 2. Applied transformer models: a) single-phase transformer  $S = 100$  MVA, b) three-phase transformer  $S = 120$  MVA

In Equation (2) – (6) capital letters denote quantities in the frequency domain, lower-case letters denote quantities in the time domain. Bold letters denote vectors and matrices including the voltage or the current of each phase for the primary and the secondary winding system (e.g.  $\mathbf{U}(k) = [U_1(k), \dots, U_o(k)]^T$ , with  $o \dots$  total number of windings), the resistances, and the self and mutual inductances.

The primary voltages and the diagonal  $m \times m$  load reactance matrix  $\mathbf{Z}_{load}$  at the secondary windings define the transformers load:

$$\mathbf{U}_2 = -\mathbf{Z}_{load} \cdot \mathbf{I}_2. \quad (7)$$

Equation (7) is inserted into Equation (2). Discrete Fourier coefficients defines the load reactance matrix. Therefore, it is possible to calculate arbitrary periodic load cases. The transformers working point can be determined for symmetrical, unsymmetrical, and nonlinear loads.

In this paper, the winding resistances are considered constant and will be calculated analytically by the winding geometry. The inductance matrix is extracted systematically from a Finite Element model of the transformer by means of static simulations in the time domain based on the magnetic energy. The method to extract the inductance matrix is described in detail in [4]. The working point of the transformer, considering nonlinear core material, is determined as depicted in the flow chart in Figure 1.

Initially the core reluctivity is assumed constant. Therefore, the inductance matrix can be extracted by a linear finite element computation. If the transformer operates at rated voltage, the permeability value at rated flux density of the core's nonlinear B-H characteristic, is a suitable choice for this initial calculation. The initial fundamental component of the transformer currents  $\mathbf{I}(1)$  is calculated by Equation (2). By means of the inverse Fourier transformation the currents are transformed into the discrete time domain. The required maximum frequency resolution determines the minimum sample rate, taking into account the Nyquist-Shannon sampling theorem. For each time step, a nonlinear FE-computation is performed and the

secant inductance matrix is determined. Due to incipient saturation in certain areas of the core, the inductance matrix varies with the current, and therefore in time. A Fourier decomposition of the inductance matrix is performed and an updated set of transformer currents including the harmonics of the inductance matrix is calculated by Equation (2). Again, these currents will be transformed into the time domain and nonlinear inductance matrix is computed. These iteration will be repeated until the difference of the transformer currents is smaller than a defined error limit  $\varepsilon = 1\%$ .

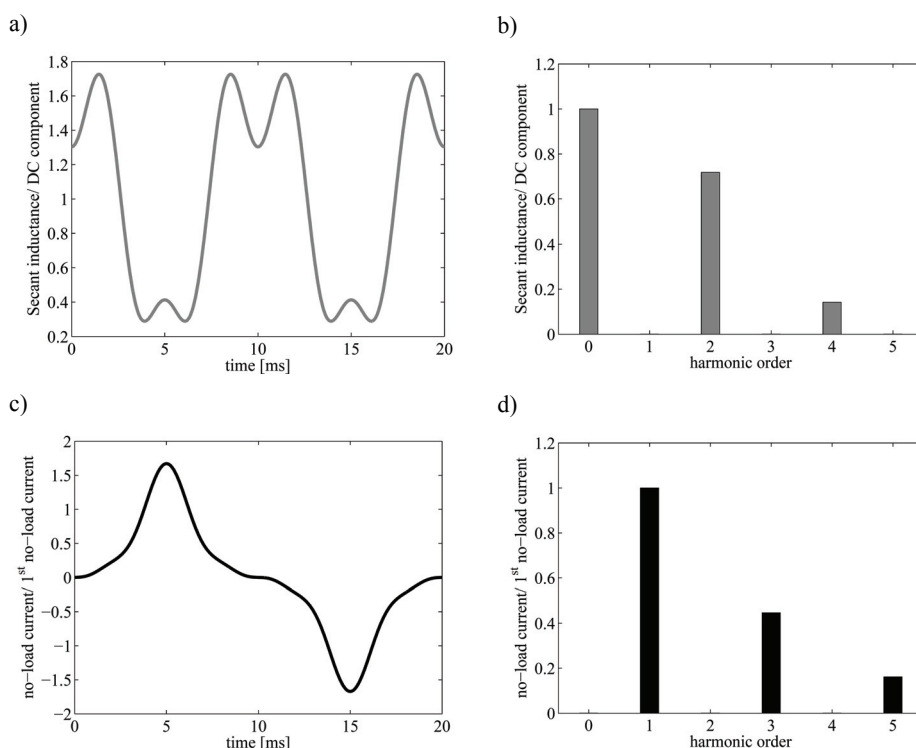


Fig. 3. No load inductance and current, single phase transformer ( $S = 100 \text{ MVA}$ ): a) time characteristic: inductance, b) harmonic contents: inductance, c) time characteristic: current, d) harmonic contents: current

The proposed method is based on a weak coupling of the electrical equation system and the FE-system. The coupling parameters are the secant inductance matrices. The number of time steps determines the number of considered harmonics. The number of harmonics influences only the size of the electrical equation system (2). The size of the FE system matrix is constant and does not depend on the number of harmonics. For a strong-coupled multi-harmonic approach, the electrical system equation and the harmonics are assembled in a single system matrix [3]. Due to the increased FE system matrix the memory limit of the PC will be a limiting factor, especially for analysis by means of large three-dimensional FE models.

For the proposed approach the secant inductance matrices are determined for each time-step by a static nonlinear FE computation based on the magnetic vector potential with the cur-

rent shape functions as excitation. For this case, the symmetric Finite Element system matrix is good conditioned and it assures a good convergence for the nonlinear Newton Raphson iterations. Because the different time-steps of the nonlinear FE computation are independent from each other, the single time-steps can be computed in parallel. By parallelisation, the computational effort is constant, but the overall simulation time reduces further. The speed up is nearly linear.

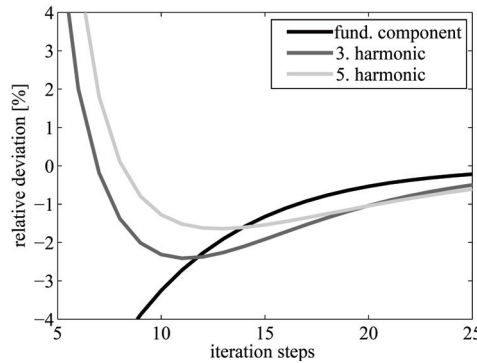


Fig. 4. Convergence behaviour of the multi-harmonic calculation

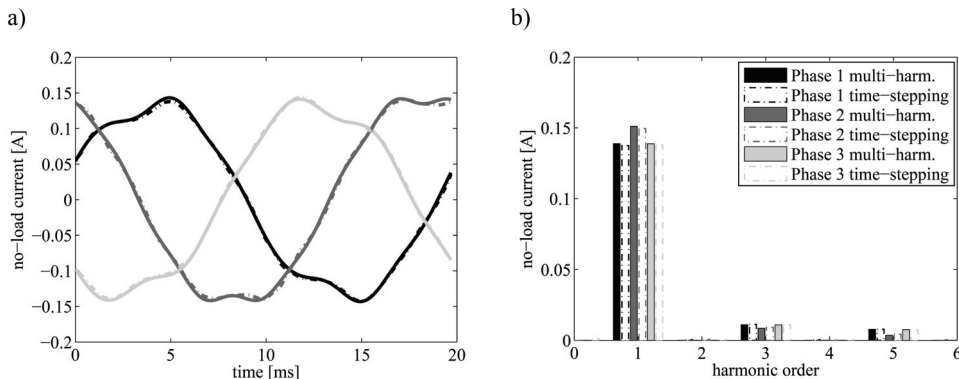


Fig. 5. No load currents, Three-phase transformer ( $S = 120$  MVA): a) time characteristics: inductance,  
b) harmonic contents: inductance

### 2.1. Application

The proposed method is applied to a 3D Finite Element model of a single-phase transformer and a 2D Finite Element model of a five-limb three-phase transformer. The single-phase transformer, depicted in Figure 2a), is rated at  $S = 100$  MVA with a rated voltage at  $U = 220$  kV. The three-phase transformer, depicted in Figure 2b), is rated at  $S = 120$  MVA with a phase-to-phase voltage of  $U = 220$  kV. The no load operation is calculated for both transformer types. The no load current and the self-inductance of the primary winding are plotted in Figure 3 for the single-phase transformer. A pure sinusoidal voltage at fundamental frequency  $f = 50$  Hz excites the transformer. Due to incipient saturation of the core material,

odd harmonics occur in the spectrum of the inductance. For a pure sinusoidal voltage, these harmonics induce even harmonics in the current spectrum.

The finite element model of the single-phase transformer has 90000 elements. Defining a sample rate of 16 for the time discretisation the 7<sup>th</sup> harmonic of the currents is resolved. One iteration step (it) has a computational effort of 20 minutes. The inductance matrix is calculated by static FE computations, and the time steps are independent from each other. Therefore, it is possible to reduce the computational time per iteration by parallelisation of the different time steps. The computation time reduces to 1.25 minutes per iteration for the given 3D FE model.

Figure 4 depicts the convergence behaviour of the proposed method. The error of the current values decreases with an increased iteration step. At iteration step 15, the difference of the fundamental component between two iteration steps is smaller than 1%. The difference of the third and fifth harmonic is smaller than 1% at iteration step 25.

A comparison with a time-stepping method is performed for the three-phase transformer. Figure 5 depicts the no load currents' time characteristic and the harmonic contents. The no load current and the harmonic contents are in good agreement. The maximum relative deviation of the fundamental component is less than 1%. The computational effort decreases significantly for the multi-harmonic approach. The computational effort of the multi-harmonic approach is approximately 30 minutes (w/o parallelisation), whereas the effort of the time-stepping method is more than 2 days, due to the transient phenomenon [4].

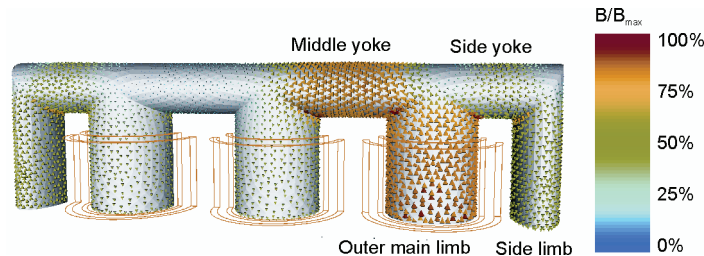


Fig. 6. Flux distribution inside the five-limb three-phase power transformer core (3D FEM)

### 3. Load dependent flux variations

Phase-shifting transformers (PSTs) are used to control the real power flow in transmission lines. A PST injects a voltage between its source and load side terminals that is in quadrature to the phase-to-ground voltage of the system. Therefore, the load current through the coil pairs of PSTs has a phase shift of close to  $\pm 90^\circ$  relative to the exciting voltage of the transformer or transformer pair, which is equivalent to a capacitive or inductive load of a regular transformer. Due to the superposition of exciting- and stray-flux significant local variations of the core fluxes may occur. The highest local fluxes in the core(s) of a PST are encountered when the PST is used to oppose the “natural” power flow through a transmission line, i.e. in “retard” operation [5].

In this section, this operation mode is modelled by a capacitive load case at rated power, for the 120 MVA five-limb three-phase transformer. The outer winding system is excited by a line-to-line voltage  $U = 220$  kV. The inner winding system is connected to the capacitive load. Both winding systems have a grounded neutral. The multi-harmonic approach is applied to calculate the flux distribution by means of a 2D FE-model, see Figure 2(b), and a 3D FE-model, Figure 6. To visualize local flux variations, the flux respectively the flux density of the capacitive load case is related to the no-load flux-density distribution in Figure 7. Flux variations are depicted for the side yoke, middle yoke, side limb, and outer main limb. Figure 6 depicts the flux density inside the core at the time-instance of maximum flux in the outer main limb, and defines the core members.

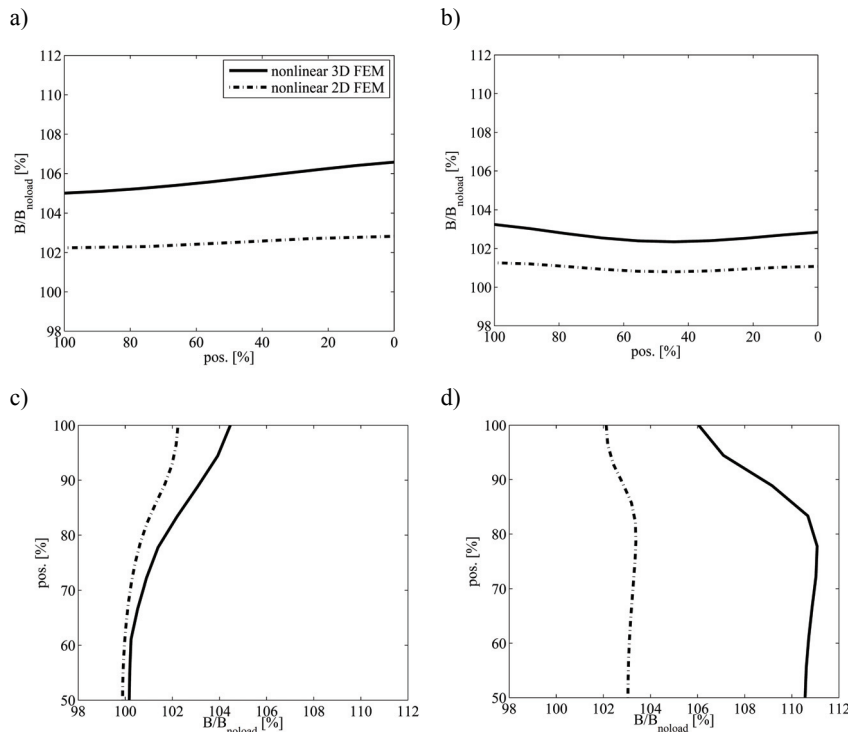


Fig. 7. Flux variations inside the transformer core due to capacitive load (fundamental component):  
a) side yoke, b) middle yoke, c) side limb, d) outer main limb

Due to superimposed stray fluxes in phase with the main flux, the flux density inside the core increases. The maximum flux variation for the 3D FE model is 11%, which is in good agreement with the relative short circuit impedance of the transformer. The deviations of the flux variation, when compared with the 2D FE model are significant. In a 2D FE model, no 3D-effects, e.g. magnetic fluxes that close outside the cross-sectional area, can be considered. Dependent on the depth (dimension perpendicular to the cross-sectional area), the main flux or

the load dependent stray flux can be represented [5]. To assure a comparable saturation state of the core in 2D and 3D the depth is determined by the way, that the core cross-sectional area of the 2D model is equal to the real transformers core-cross sectional area ( $d_{2D} = \pi \cdot d_{core} / 4$ ). The stray flux for this 2D simulation is underestimated. The maximum flux deviation between the no load and capacitive load case is 3.5%. For the case, which defines the depth of the 2D model by:  $d_{2D} = \pi \cdot d_m / 2$  ( $d_m$  ... mean winding diameter), the amount of stray flux can be considered by the 2D model, but the limb cross sectional area will increase and therefore the saturation state will be erroneous. From this comparison it can be stated, that a 3D model is necessary if nonlinear material properties of the transformer core are taken into account.

Figure 8 shows the harmonic contents of the magnetic flux at the different core members. Inside the main limb, the flux is purely sinusoidal, due to the applied sinusoidal voltage no higher harmonics of the flux occur. Due to the five-limb structure a third harmonic of the flux occurs, for incipient saturation at the middle limb. This flux component closes its path over the middle yoke, side yoke and side limbs. The magnitude of the flux is 7.8% at the middle yoke, respectively 12.3% at the side yoke.

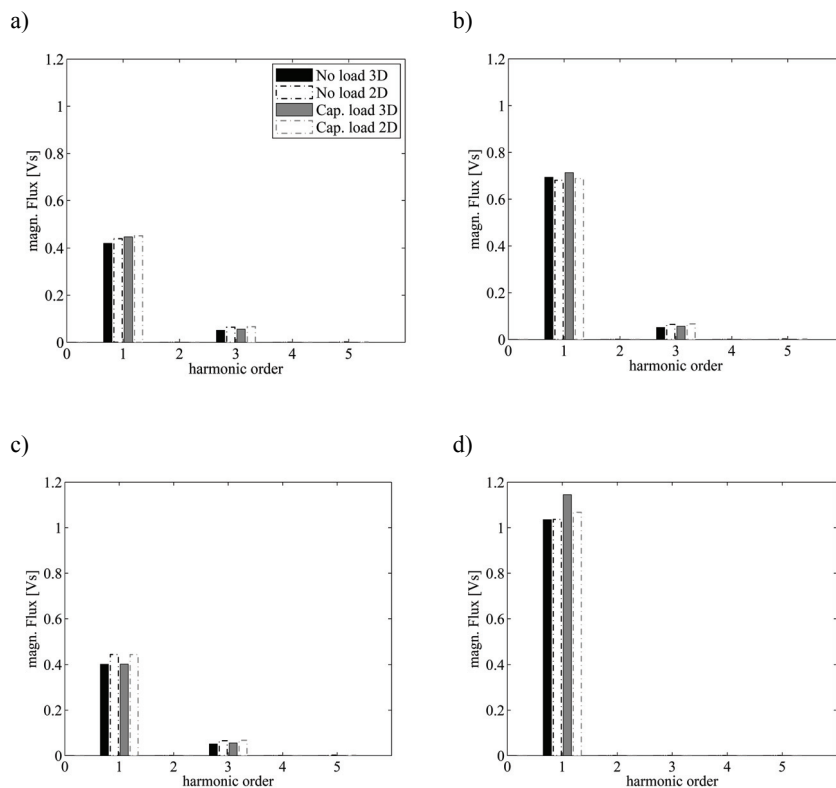


Fig. 8. Flux distribution capacitive load: harmonic contents: a) side yoke, b) middle yoke, c) side limb, d) outer main limb

#### 4. Conclusions

This paper presents a methodology for the calculation of the flux distribution in power transformer cores considering nonlinear material with reduced computational effort. The calculation is based on a weak coupled multi-harmonic approach. The methodology can be applied to 2D and 3D Finite Element models. The load dependent inductance matrix is calculated by static FE simulations in the time domain, whereas the electrical equation system of the transformer is solved in the frequency domain.

The savings of the proposed approach compared to a time-stepping method is >90% at comparable accuracy. Furthermore, the approach offers a possibility for parallelisation to reduce the overall simulation time. The speed up of the parallelised simulations is nearly linear.

The methodology is exemplary applied to a single-phase and three-phase transformer. The determination of the working point using a 3D nonlinear FE model takes about 30 minutes. A comparison of the flux distribution for capacitive load is performed between the calculation by means of a 2D and 3D FE model. Deviations of the 2D FE model compared to the 3D FE model are significant, due to the fact, that the 2D FE model underestimates the stray fluxes. If the non-linearity of the core material has to be taken into account a 3D FE model is required.

For the capacitive load case the flux in the main limb increases by 11%, which is in good agreement with the relative short circuit impedance of the inspected transformer. For the five-limb design a third harmonic due to incipient saturation in the flux is identified at the middle yoke, side yoke and respectively the side limbs.

#### References

- [1] Vassent E., Meunier G., Sabonnadier J., *Simulation of induction machine operation using complex magnetodynamic finite elements*. IEEE Transactions on Magnetics 25(4): 3064-3066 (1989).
- [2] Yamada S., Bessho K., Lu J., *Harmonic balance finite element method applied to nonlinear AC magnetic analysis*. IEEE Transactions on Magnetics 25(4): 2971-2973 (1989).
- [3] De Gersem H., Vande Sande H., Hameyer K., *Strong coupled multi-harmonic finite element simulation package*. COMPEL: The International Journal for Computation and Mathematics in Electrical and Electronic Engineering 20(2): 535-546 (2001).
- [4] Riemer B., Lange E., Hameyer K., *Calculation of the flux distribution of three phase five limb power transformers considering nonlinear material properties*. COMPEL: The International Journal for Computation and Mathematics in Electrical and Electronic Engineering 32(4): 1230-1243 (2013).
- [5] Riemer B., Bonmann D., Hameyer K., *Flux distribution in transformer cores of Phase-Shifting transformers*. CIGRE SC A2 & C4 Joint Colloquium 2013, Zurich (2013).